Liquid Crystals
Publication details, including instructions for authors and subscription information:
http://www.informaworld.com/smpp/title~content=t713926090

Deformed helix ferroelectric liquid crystal display: A new electrooptic mode in ferroelectric chiral smectic C liquid crystals

L. A. Beresnev[a]; V. G. Chigrinov[b]; D. I. Dergachev[a]; E. P. Poshidaev[b]; J. Fünfschilling[c]; M. Schadt[c]
[a] Shubnikov's Crystallography Institute, Moscow, U.S.S.R. [b] Organic Intermediates and Dyes Institute, Moscow, U.S.S.R. [c] Central Research Units, F. Hoffmann-La Roche & Co. Ltd, Basel, Switzerland

To cite this Article Beresnev, L. A. , Chigrinov, V. G. , Dergachev, D. I. , Poshidaev, E. P. , Fünfschilling, J. and Schadt, M.(1989) 'Deformed helix ferroelectric liquid crystal display: A new electrooptic mode in ferroelectric chiral smectic C liquid crystals', Liquid Crystals, 5: 4, 1171 — 1177

To link to this Article: DOI: 10.1080/02678298908026421

URL: http://dx.doi.org/10.1080/02678298908026421

Liquid Crystals, 1989, Vol. 5, No. 4, 1171–1177

Deformed helix ferroelectric liquid crystal display: a new electrooptic mode in ferroelectric chiral smectic C liquid crystals

by L. A. BERESNEV†, V. G. CHIGRINOV‡, D. I. DERGACHEV†,
E. P. POSHIDAEV‡, J. FÜNFSCHILLING§ and M. SCHADT§

† Shubnikov's Crystallography Institute, 117333, Moscow, U.S.S.R.
‡ Organic Intermediates and Dyes Institute, 103787, Moscow, U.S.S.R.
§ F. Hoffmann-La Roche & Co. Ltd, Central Research Units,
CH-4002 Basel, Switzerland

A new electrooptic mode of operation of ferroelectric chiral smectic C liquid crystal displays (LCDs) is proposed and demonstrated. The effect, which is called the deformed helical ferroelectric (DHF) effect, is based on the deformation of the helical structure by weak electric fields. In the unbiased device the smectic layers are arranged in the bookshelf geometry with the helix axis parallel to the electrodes [1]. Systems with a very small pitch ($< 1\,\mu$m) and a large tilt angle are especially well suited for this mode. The key characteristics of DHF-LCDs are: (*a*) low driving fields ($1\,V_{p-p}\,\mu m^{-1}$ for maximum contrast); (*b*) grey scale which is approximately linear with the applied electric field; (*c*) easy alignment even for thick cells using standard wall-aligning methods; and (*d*) response times at room temperature of $300\,\mu$s.

1. Introduction

In 1980 Clark and Lagerwall proposed a new electrooptic switching in a surface stabilized geometry, distinguished by a high optical contrast and fast operation speed [1]. Subsequent papers contributed to the different aspects of the Clark–Lagerwall effect, such as operation speed and contrast dependence on the physical parameters of S_C^* and the boundary treatment [2–4], the occurrence of bistable and memory states due to the boundary conditions [5–8], the effect of defects and the character of disclination lines [9, 10], the efficiency of the electronic driving circuits [11, 12], etc. However, progress in the wide application of the Clark–Lagerwall effect is still too slow because of the crucial dependence of its characteristics on the surface treatment, the absence of a natural grey scale, the complicated physics of the memory state origin, and so on. Solutions to these problems would result in an unpredictable growth of the number of ferroelectric liquid crystal devices, possessing both the multiplexing capability and a high speed of operation.

In this paper we propose another electrooptic mode in ferroelectric chiral smectic C liquid crystals, which we call the deformed helix ferroelectric liquid crystal display (DHF-LCD) mode. This mode has been mentioned previously [13–16], but has now become very important because of the success in developing new ferroelectric liquid crystals with large smectic tilt angles, Θ_0, and low helix pitch values, P_0. Application of this mode in electrooptic displays will provide a fast operation speed at low voltages, linear or quadratic intensity–voltage dependence (grey scale), insensitivity to surface treatment, etc. Our first attempts to adapt this electrooptical mode to a practical application in liquid crystal light valves proved to be very promising [17].

0267–8292/89 $3.00

2. Theory

The preferred geometry of the DHF-LCD is as follows. The conventional planar sandwich cell contains a chiral smectic C liquid crystal with its helix axis oriented parallel to the substrates (see figure 1). The polarizer (P) on the first substrate makes an angle β with the S_C^* helix axis and the analyser (A) is crossed with the polarizer. The chiral smectic C layers are perpendicular to the substrates, the cell gap is several times higher than the S_C^* helix pitch. The light beam with the aperture $a \gg P_0$ passes parallel to the chiral smectic C layer through the S_C^* sample, placed between the polarizer and the analyser.

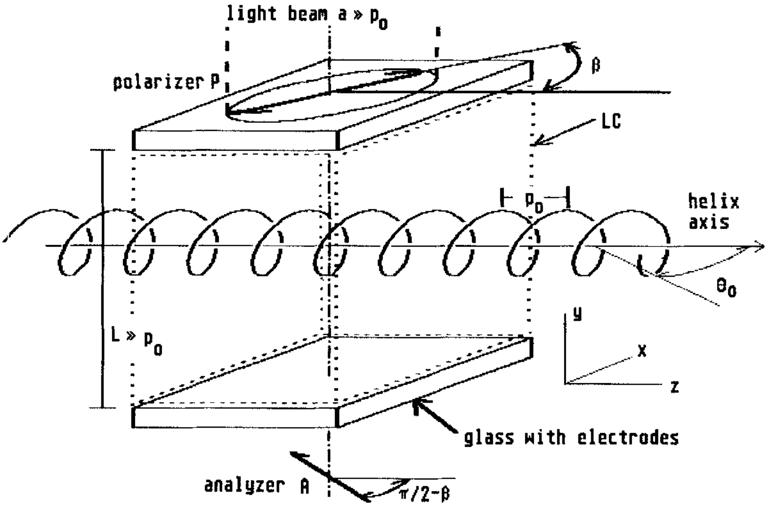

Figure 1. Deformed helix ferroelectric liquid crystal display. The light with the aperture $a \gg P_0$ passes through the polarizer (P), DHF-cell (P_0 is the helix pitch, z is the helix axis and Θ_0 is the S_C^* director tilt angle) and analyser (A) crossed with polarizer. Smectic layers are perpendicular to the substrates, A.C. voltage U is applied parallel to the formers. β is the angle between the polarizer P and the helix axis z.

The behaviour of the DHF structure in an electric field has been described [14–16], including its static [14] and dynamic [15, 16] aspects. Far from the phase transition to the chiral smectic C the variations of the smectic tilt angle, Θ_0, in the electric field become energetically unfavourable and only the rotation angle φ around the helix axis is modulated. The corresponding dependence of the molecular distribution $\cos\varphi(Z')$ (where $Z' = 2\pi Z/P_0$) oscillates symmetrically in $\pm E$ electric fields (see figure 2). These oscillations result in variation of the effective refractive index n of the S_C^*; the index ellipsoid is tilted and deformed by the electric field.

This situation occurs up to fields E near the unwinding value E_u [9, 18]:

$$E_u = \frac{\pi^2}{16}\frac{Kq_0^2}{P_c}, \tag{1}$$

where $K = K'\theta_0^2$ is the effective elastic coefficient, Θ_0 is the smectic C* tilt angle, $q_0 = 2\pi/P_0$ is the wavevector corresponding to the unperturbed pitch P_0, $P_c = \eta_\perp\mu_p\Theta_0$ is the piezoelectric polarization of the S_C^* ($\eta_\perp$ is the susceptibility, μ_p is the piezomodule). According to equation (1) the range of the voltages used in

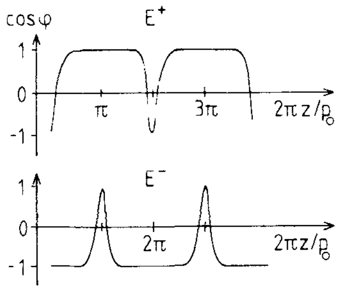

Figure 2. Variation of the director distribution $\cos\varphi$ (z', E) in the xy plane (see figure 1) for the electric voltage $U = 0{\cdot}99U_c$. φ is the rotation angle of the director around the z axis.

DHF-LCD mode $U = EL$ widens with increasing L/P_0 ratio:

$$\left.\begin{aligned} 0 &\leqslant U \leqslant U_u, \\ U_u &= E_u L \\ &= \frac{\pi^4}{4}\frac{K}{LP_c}\left(\frac{L}{P_0}\right)^2. \end{aligned}\right\} \qquad (2)$$

At the same time the helix pitch, P, remains approximately equal to P_c within the entire range of the applied voltages $0 \leqslant U \leqslant U_u$ (see figure 3).

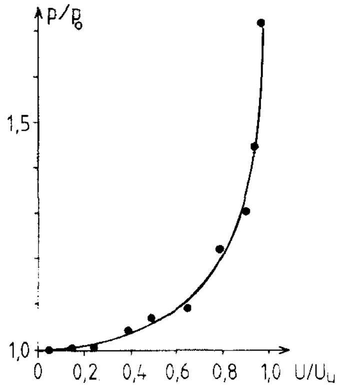

Figure 3. Dependence of the reduced helix pitch, P/P_0, of the DHF-LCD on the relative voltage, U/U_u, where U_u is the helix unwinding voltage [14–16].

In a linear approximation the S_C^* director rotation angle varies in the electric field $\mathbf{E} = \mathbf{E}_0 \cos\omega t$ as follows [14–16]:

$$\begin{aligned} \varphi &= z' + A\sin z' \\ &= z' + \frac{\alpha}{1 + (\omega/\omega_c)^2}\left(\cos\omega t + \frac{\omega}{\omega_c}\sin\omega t\right)\sin z', \qquad (3) \\ \alpha &= \frac{\pi^2}{16}\frac{E}{E_u} \quad E < E_u \end{aligned}$$

is the relative field amplitude,

$$\omega_c = \frac{K'\Theta_0^2 q_0^2}{\gamma_\varphi}$$

is the characteristic frequency and γ_φ is the viscosity of the twist (φ) deformations of the S_C^* director, and

$$z' = 2\pi z/P \approx 2\pi z/P_0.$$

In the field free case, one axis of the effective refractive index (averaged over many turns of the pitch) is parallel to the helix axis. If we denote the angle of this axis with the helical axis by χ, then $\chi = 0$ for $E = 0$ and increases or decreases to $\chi = \pm\Theta_0$ for fields larger than $\pm E_u$. For small fields χ is proportional to E. In addition to this rotation of the index ellipsoid, $|\Delta n|$ also changes; it increases linearly from its minimum value when $E = 0$ and saturates at its maximum when $|E| > E_u$. Depending on the position of the polarizer (β in figure 1), the light changes quadratically ($\beta = 0$) or linearly with E (β adjusted such that the transmitted intensity is half its maximum for $E = 0$, i.e. $\pi/8$).

In the small signal limit the time constant of the light modulation is the same as in equation (3), namely

$$\tau_c = \omega_0^{-1} = \frac{\gamma_\varphi}{K'\Theta_0^2 q_0^2}. \tag{4}$$

For $K' \approx 10^{-6}$ dyn, $\gamma_\varphi \approx 1$ P, $\Theta_0 \approx 29°$ and $P_0 = 2\pi/q_0 \approx 0{\cdot}5\,\mu$m we have $\tau_c \approx 250\,\mu$s and it decreases sharply for the lower P_0 values as P_0^2. The slow dependence of the helix pitch P on the applied voltage (see figure 3) means that the response times of DHF-LCDs are practically independent of voltage up to the unwinding voltage.

If the voltage U approaches the unwinding value U_u, the pitch P increases sharply and the relaxation times for the distorted helix to its initial state t_r become very large [15] (see figure 4):

$$\frac{t_r}{\tau_c} \approx \frac{P^2}{P_0^2}. \tag{5}$$

From this it is evident that in DHF-LCDs it is possible to implement a voltage controllable memory state.

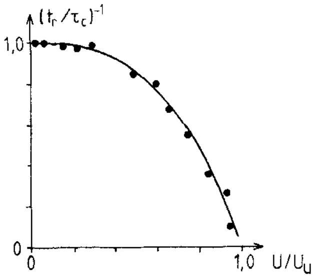

Figure 4. The inverse of the reduced relaxation time t_r/τ_c of the DHF-LCD versus the relative applied voltage U/U_u. U_u is the helix unwinding voltage, τ_c is the characteristic response time (equation (4)).

3. Experiment

Experimental data confirm the validity of our theoretical considerations of DHF-LCD mode. In our experiment we have used two mixtures: A and B. These mixtures were produced from a low viscosity and broad temperature range non-chiral smectic C and a mesogen or non-mesogen chiral additive with high spontaneous polarization. One of these chiral additives, which we called Luch-15, has remarkable properties: high spontaneous polarization (3 to 5 × $10^{-7}\,\mathrm{C\,cm^{-2}}$), good solubility (about 35 wt %) in the S_C mesogen, which provides small values of the helix pitch, P_0 (about 0·3–0·4 μm), acceptable orientation order and low viscosity values. Using Luch-15 and different smectic C materials, we have obtained the parameters for ferroelectric liquid crystals for the DHF-LCD mode shown in the table.

Ferroelectric liquid crystals for the DHF-LCD mode.

Parameter	Mixture A	Mixture B
Helix pitch, $P_0/\mu\mathrm{m}$ at 25°C	0·3–0·4	0·3–0·35
Tilt angle, $\Theta_0/°$ at 25°C	29	30
Working temperature range/°C	8–54	2–50·5
Polarization, $P_s/10^{-8}\,\mathrm{C\,cm^{-2}}$	7	8
Unwinding voltage, U_u/V	2 ± 0·1	3 ± 0·1
Layer thickness, $L/\mu\mathrm{m}$	3·3 ± 0·1	10 ± 0·2
Effective birefringence, Δn	0·10	0·11
Response time/μs		
at U = 1·5 V	150–200	
at U = 2 V		500

Figure 5 shows the transmission–voltage dependence (grey scale) of (*a*) linear and (*b*) quadratic modes (mixture B). The transmission increases linearly with (*a*) voltage and (*b*) as the square of the voltage, complying with the theoretical predictions.

Figure 6 shows the frequency dependence of the modulation amplitude $I(\omega)$ in a DHF-LCD for the linear mode. The predicted law derived from equation (3), $I(\omega) \approx I_0\,[1 + (\omega/\omega_c)^2]^{-1/2}$ (I_0 = constant) fits the experimental data to a high accuracy for $f_c (= \omega_c/2\pi)$ = 800 Hz (mixture B).

Memory effects near the unwinding voltage $U \approx U_u$ have also been observed. The inverse time $(t_r/\tau_c)^{-1}$ approaches zero for voltages U close to the unwinding value U_u for $U \lesssim U_u$ (see figure 4). The physical origin of the memory effects is clear: the deformed helix accumulates some small amount of elastic energy, which is responsible for winding the helix to the initial state. However, some details of the process are not well understood yet, and further investigations are needed.

Figure 7 shows the intensity of the transmitted light versus the cell thickness for $U < U_u$ and $U > U_u$ (mixture B). The experiment was carried out in a wedge-shaped

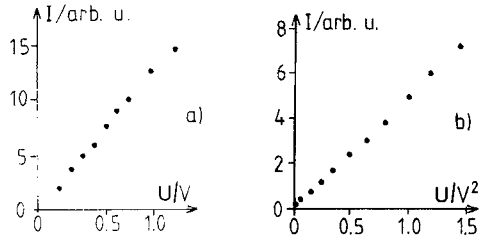

Figure 5. Voltage dependence of the transmission (*a*) linear and (*b*) quadratic modes, measured for the mixture B.

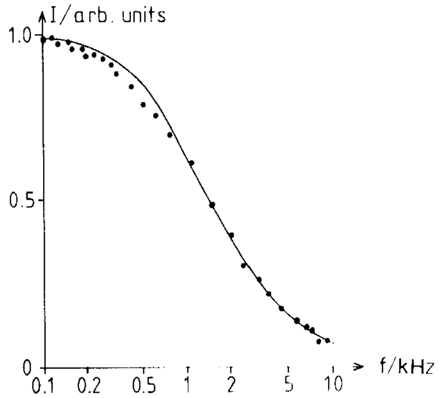

Figure 6. The frequency dependence of the modulation amplitude of the linear mode. The solid line indicates the law $I \approx I_0[1 + (\omega/\omega_c)^2]^{-1/2} = I_0[1 + (f/f_c)^2]^{-1/2}$ derived from equation (3), for $f_c = 800\,\mathrm{Hz}$.

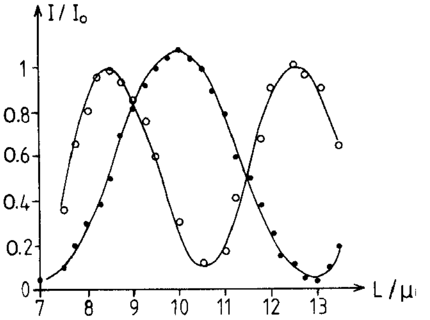

Figure 7. Light transmission versus the thickness L of the liquid crystal layer in a wedge cell for (●) $U < U_u$ and (○) $U > U_u$.

cell. The advantage of the DHF-LCD mode for $U < U_u$ reveals itself in the smoother dependence of the transmittance on layer thickness over the display working are. The experiment confirms that

$$\Delta n_{\mathrm{DHF}}(U < U_u) < \Delta n_{\mathrm{max}}(U > U_u).$$

For Δn we obtain from figure 7: $\Delta n \approx 0{\cdot}16$ for $U > U_u$ and $\Delta n \approx 0{\cdot}11$ for $U < U_u$.

The DHF-LCD provides fast operation for relatively low voltages. Estimates of the response time were made by two different methods. In the first method we defined the time of the DHF-LCD response to square-wave voltage excitation (10 per cent + 90 per cent intensity level), whereas the second method was based on measurement of the characteristic frequency $f_c = \omega_c/2\pi$ for a harmonic field excitation (see figure 6). Good agreement of the response data, obtained by these different methods, was observed. The results are given in the table.

The experiments have revealed the following features of the DHF-LCD response times.

(*a*) The response time does not depend on the voltage amplitude $U < U_u$, layer thickness $L \gg P_0$ or smectic C* polarization value P_c. The only important parameter are the unperturbed helix pitch P_0, the smectic C* twist elastic constant $K = K'\Theta_0^2$ and the rotational viscosity γ_φ (see equation (3)).

(*b*) For relatively low voltages the intensity modulation is obtained by a slight variation of the chiral smectic C director distribution near the unpertubed state. Consequently, the instantaneous response of the system is provided without the so-called delay time, as in the Clark–Lagerwall effect [2], where the initial torque on the director is small.

(*c*) The DHF-LCDs are also less sensitive to the surface treatment and to layer thickness variations within the surface working area of the display than the Clark–Lagerwall effect [1]. This is very good from the point of view of their applicability. The insensitivity of the DHF-LCD to the surface treatment enables us to utilize successfully common aligning techniques for producing homogeneous alignment on the substrates: rubbing, oblique evaporation etc. High quality orientation is easily obtained, which provides a contrast ratio of up to 100 : 1 or even more.

In conclusion we note that the main advantages of the new electro-optical mode make it competitive with the Clark–Lagerwall effect in some applications, such as low voltage, quick response light modulators, image transducers, liquid crystal light valves [16], etc.

References

[1] Clark, N. A., and Lagerwall, S. T., 1980, *Appl. Phys. Lett.*, **36**, 899.

[2] Xue Jiu-Zhi, Handschy, M. A., and Clark, N. A., 1987, *Ferroelectrics*, **73**, 305.

[3] Schiller, P., 1986, *Crystal Res. Technol.*, **21**, 301.

[4] Barnik, M. I., Baikalov, V. A., Chigrinov, V. G., and Poshidaev, E. P., 1987, *Molec. Crystals liq. Crystals*, **143**, 101.

[5] Schiller, P., Pelzl, G., and Demus, D., 1987, *Liq. Crystals*, **2**, 21.

[6] Hatano, T., Yamamoto, K., Takezoe, H., and Fukuda, A., 1986, *Jap. J. appl. Phys.*, **25**, 1762.

[7] Handschy, M. A., and Clark, N. A., 1983, *Ferroelectrics*, **59**, 69.

[8] Patel, J. S., 1985, *Appl. Phys. Lett.*, **47**, 1277.

[9] Glogarova, M., and Pavel, J., 1984, *J. Phys., Paris*, **45**, 143.

[10] Clark, N. A., and Lagerwall, S. T., 1986, *Proceedings 6th International Display Research Conference 'Japan Display '86'*, Tokyo, Japan, 1986, p. 456.

[11] Shimoda, S., Ito, K., Harada, T., Taguchi, M., Iwasa, K., and Kai, M., 1986, *Proceedings 6th International Display Conference 'Japan Display '86'*, Tokyo, Japan, 1986, p. 460.

[12] Geary, J. M., 1985, *SID 85 Dig.*, p. 128.

[13] Yoshino, K., Balakrishnam, K. G., Uemoto, T., Ywasaki, Y., and Inuishi, Y., 1987, *Jap. J. appl. Phys.*, **17**, 597.

[14] Ostrovski, B. I., and Chigrinov, V. G., 1980, *Kristallografiya*, **25**, 560.

[15] Ostrovski, B. I., Rabinovich, A. Z., and Chigrinov, V. G., 1980, *Advances in Liquid Crystal Research and Applications*, edited by L. Bata (Pergamon Press–Adademiai Kiado), p. 469.

[16] Chigrinov, V. G., Baikalov, V. A., Poshidaev, E. P., Blinov, L. M., Beresnev, L. A., and Allaguloy, A. I., 1985, *Soviet Phys. JETP*, **61**, 1193.

[17] Beresnev, L. A., Blinov, L. M., and Dergachev, D. I., 1987, *1st International Symposium of Ferroelectric Liquid Crystals*, Bordeaux, France, 1987, Abstracts, p. 62.

[18] Glogarova, M., Lejĉek, L., Pavel, J., Janoves, V., and Fousek, J., 1983, *Molec. Crystals liq. Crystals*, **91**, 309.

[19] Rokushima, K., and Yamakita, J., 1987, *J. opt. Soc. Am.* A, **4**, 27.